

## Supporting Information

# Enabling Rechargeable Non-aqueous Mg-O<sub>2</sub> Battery Operations with Dual Redox Mediators

Qi Dong, Xiahui Yao, Jingru Luo, Xizi Zhang, Hajin Hwang, Dunwei Wang\*

Department of Chemistry, Merkert Chemistry Center, Boston College, 2609 Beacon Street, Chestnut Hill,  
Massachusetts 02467, United States

## Table of Contents

1. Experimental section
2. Table 1. Potential redox mediators (RMs) from the literature
3. Fig. S1 Cyclic voltammetry (CV) of various analytes with supporting salt of TBAPF<sub>6</sub>
4. Fig. S2 Home-designed electrochemical cell for the three-electrode measurements
5. Fig. S3 Cyclic voltammetry (CV) to calibrate the Mg ribbon as the pseudo reference electrode
6. Fig. S4 Analyte screening with home-designed electrochemical cell
7. Fig. S5 Cyclic voltammetry (CV) of Mg electrode in Mg(ClO<sub>4</sub>)<sub>2</sub>/DMSO
8. Fig. S6 Cyclic voltammetry (CV) of BQ in Mg(ClO<sub>4</sub>)<sub>2</sub>/DMSO
9. Fig. S7 Galvanostatic cycling using reduced concentrations of RMs
10. Fig. S8 Cycling performance in RMs-free Mg(ClO<sub>4</sub>)<sub>2</sub>/DMSO using a Swagelok cell in a two-electrode configuration
11. Fig. S9 Galvanostatic cycling plotted by capacity-cutoff
12. Fig. S10 SEM images and EDS spectra of the carbon paper cathode after deep discharge
13. Fig. S11 XRD patterns of carbon paper cathodes after different operations
14. Fig. S12 NMR spectra of electrolytes before and after cycling
15. Fig. S13 XPS C 1s spectra of carbon paper cathodes after different operations
16. Fig. S14 SEM images of the Mg anodes after different operations in Mg(ClO<sub>4</sub>)<sub>2</sub>/DMSO electrolyte
17. Fig. S15 Pressure change during discharge and recharge
18. References

## Experimental Section

**Chemicals and materials:**  $\text{Mg}(\text{ClO}_4)_2$  (ACS reagent grade),  $\text{MgCl}_2$  (ACS reagent grade),  $\text{LiClO}_4$  (battery grade), 1,4-benzoquinone (BQ,  $\geq 99.5\%$ ), 5,10,15,20-tetraphenyl-21H,23H-porphine cobalt(II) (Co(II)TPP,  $\geq 85\%$ ), tetrabutylammonium hexafluorophosphate ( $\text{TBAPF}_6$ ,  $\geq 99.0\%$ ), ferrocene (Fc, 98%), magnesium peroxide complex ( $\text{MgO}_2 \cdot x\text{MgO}$ ,  $\text{MgO}_2$ , 24-28%), dimethyl sulfoxide (DMSO, anhydrous grade), 1,2-dimethoxyethane (DME, anhydrous grade), N,N-dimethylacetamide (DMA, anhydrous grade) were purchased from Sigma-Aldrich. Deuterated  $\text{CDCl}_3$  (99.8%) was purchased from Cambridge Isotope Labs.  $\text{Mg}(\text{TFSI})_2$  was purchased from Solvionic and dried for 2 days at 240 °C under vacuum. All solvents were further dried by 4Å molecular sieves prior to use. Mg ribbon ( $\geq 99\%$ , trace metals basis, Sigma-Aldrich) was polished with a blade and sand paper to remove the surface oxidation layer before use. Carbon paper (Toray 120) cathode was purchased from the Fuel Cell Store and cleaned by acetone, methanol and isopropanol sequentially, then dried under vacuum at 120 °C overnight before use.

**Electrochemical measurements:** All electrochemical tests were carried out using a home-designed electrochemical cell with three-electrode configuration. The cell was equipped with two glass chamber connected by a glass-frit (fine grade; thickness: 2 mm; diameter: 1 cm). The glass-frit was applied to minimize the possible crossover of the redox mediators (RMs) and anions. 0.1 M  $\text{Mg}(\text{TFSI})_2$  and 0.1 M  $\text{Mg}(\text{ClO}_4)_2$  were dissolved in DMSO as catholyte and anolyte respectively ( $\text{Mg}(\text{TFSI})_2/\text{DMSO}$ ,  $\text{Mg}(\text{ClO}_4)_2/\text{DMSO}$ ). 0.1 M  $\text{TBAPF}_6$  was dissolved in DMSO as supporting salt for control experiments ( $\text{TBAPF}_6/\text{DMSO}$ ). For cyclic voltammetry (CV) measurements, 2 mM of redox species was applied in the catholyte. For galvanostatic cycling test, the concentration of BQ and Co(II)TPP in the catholyte were optimized to be 50 mM and 5 mM respectively. Two polished Mg ribbons were immersed into the anolyte as the counter and pseudo reference electrode respectively. Pt wire ( $d=0.25$  mm) was used as working electrode for the standard CV tests. Carbon paper was placed into the catholyte as the working electrode for galvanostatic cycling measurements. The immersed area was confined to 1.0  $\text{cm}^2$  in this study. The volume of the catholyte and anolyte were both 2 mL. The cell was capped with rubber stopper and further sealed with vacuum grease after assembly. For the CV measurement, scan rate was confined to 25 mV/s. For the galvanostatic cycling measurements, the current densities were confined to 0.02  $\text{mA}/\text{cm}^2$  for both discharge and recharge. The absolute capacity was limited to 0.06 mAh (operating for 3 hours). All electrochemical tests were performed in Ar-filled (Mbraun,  $\text{O}_2$  and  $\text{H}_2\text{O}$   $< 0.1\text{ppm}$ ) or Ar-filled/ $\text{O}_2$ -tolerant glovebox (Mbraun,  $\text{H}_2\text{O}$   $< 0.1\text{ppm}$ ) at room temperature. Customized Swagelok type cells were used for two-electrode tests and were assembled in the glove box with excess piece of polished Mg ribbon as the anode, carbon paper of 1.0  $\text{cm}^2$  area as cathode and glass microfiber (GF/F, Whatman) as separator. The Swagelok cells were tested using the potentiostats (VMP3, Biologic). The assembled electrochemical cells were also studied by the potentiostats (VMP3, Biologic) with a program (GPCL-2) to monitor the potentials of both working and counter electrode based on the three-electrode configuration. Since a more accurate and stable voltage profile can be provided from the difference between the working and counter electrode ( $E_{\text{we}}-E_{\text{ce}}$ ), the voltage profile of working electrode was then extracted by taking into account the passivation of Mg pseudo reference electrode and the averaged potential required for the anode chemistry in the discharge and recharge steps.

**Material characterization:** Scanning electron microscopy (SEM) images were taken on a JEOL 6340F microscope operating at 10 kV and 20 kV, equipped with an energy-dispersive X-ray

spectroscopy (EDS) detector. X-ray diffraction (XRD) measurements were performed on PANalytical X'Pert Pro diffractometer with Cu K $\alpha$  radiation. X-ray photoelectron spectroscopy (XPS) was performed using a K-Alpha XPS (Thermo Scientific) with an Al X-ray source (incident photon energy 1486.7 eV). Cathode and anode samples were discharged and/or further fully charged to 0.2 mAh/cm<sup>2</sup> for SEM, EDS, XRD and XPS measurements. All the extracted electrode samples after testing were soaked with DMSO for overnight to remove the salts, then washed at least 5 times using acetone and isopropanol sequentially, and finally dried under vacuum at room temperature for 24 hours prior to the characterizations. <sup>1</sup>H NMR was conducted on a 500 MHz spectrometer. All NMR chemical shifts were reported in ppm referenced to the residual solvent. The electrolytes with RMs were extracted before and after cycling and dissolved in CDCl<sub>3</sub>. Pressure monitoring test was carried out by connecting the Swagelok type cell to an airtight pressure gauge with a sensitivity of 0.1 torr (MKS, 902B Piezo). Li with pretreated surface by soaking in LiNO<sub>3</sub>/DMA (0.1 M LiClO<sub>4</sub> in DMA) solution for 24 hours was applied as counter electrode for recharge to avoid possible parasitic reactions with electrolyte and RMs. Mg ribbon was applied as the counter electrode for discharge. Carbon paper was preloaded with excess amount (over 5 mg) of the magnesium peroxide complex as cathode for recharge, the loading was examined by a microbalance (Sartorius, CPA2P). Pristine carbon paper was used as the cathode for discharge. LiClO<sub>4</sub>/DME (0.1 M LiClO<sub>4</sub> in DME) with or without 2 mM Co(II)TPP were utilized as the electrolytes for recharge. Mg(ClO<sub>4</sub>)<sub>2</sub>/DMSO (0.1 M Mg(ClO<sub>4</sub>)<sub>2</sub> in DMSO) with or without 50 mM BQ were utilized as the electrolytes for discharge. Celgard 2400 films were utilized as the separator for DME-based electrolyte while glass microfiber films were used as the separator for DMSO-based electrolyte. The measurement was conducted in an isothermal chamber. A pressure baseline in the resting stage was obtained and was subtracted to extract the absolute pressure change profile.

Table S1. Potential redox mediators (RMs) from the literature.

Potential RMs	Redox couples	Redox potentials (V vs NHE)	Reference
For discharge	BQ/BQ <sup>2-</sup>	-0.07	this work
	EV <sup>-</sup> /EV <sup>2-</sup>	-0.64	1
	DEQ <sup>+</sup> /DEQ	0.31	2
	OMAB <sup>+</sup> /OMAB	0.12	2
	TMPD <sup>+</sup> /TMPD	0.29	2
For recharge	Co(III)TPP/Co(II)TPP	0.75	3, this work
	Co(III)Pc/Co(II)Pc	1.04	4
	Fe(III)Pc/Fe(II)Pc	0.65	5
	Fc <sup>+</sup> /Fc	0.56	2
	TEMPO <sup>+</sup> /TEMPO	0.70	2
	I <sub>2</sub> /I <sup>-</sup>	0.51	2

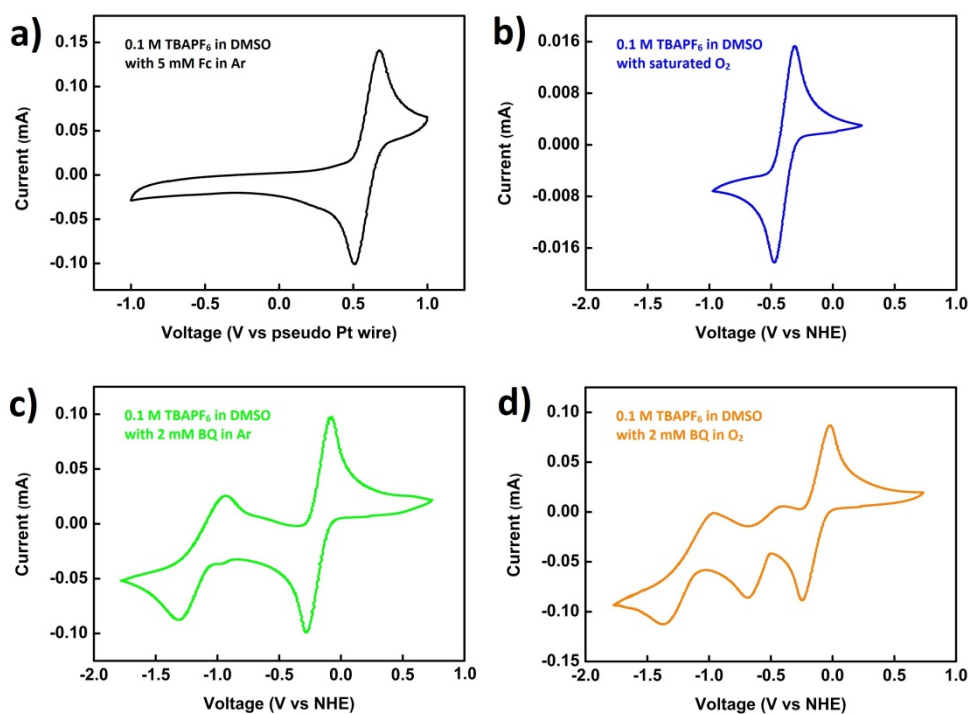


Fig. S1 Cyclic voltammetry (CV) of various analytes with supporting salt of TBAPF<sub>6</sub>. a) Calibration of pseudo Pt wire reference electrode using 5 mM Fc. b) TBAPF<sub>6</sub>/DMSO with saturated O<sub>2</sub>. c) 2 mM BQ in TBAPF<sub>6</sub>/DMSO in Ar. d) 2 mM BQ in TBAPF<sub>6</sub>/DMSO with saturated O<sub>2</sub>.

The cyclic voltammetry (CV) measurements were performed using a one-chamber cell for the ease of operation. The addition of BQ showed little influence to the counter and pseudo reference electrode thus the cell with separate chambers is not necessary. TBAPF<sub>6</sub>/DMSO (0.1 M TBAPF<sub>6</sub> in DMSO) electrolyte was applied with or without 2 mM BQ. Pt wire, polished Mg ribbon and thin Pt wire in a capillary were used as working, counter and pseudo reference electrodes respectively for this experiment. Fc<sup>+0</sup> redox couple was used as the internal reference redox pair with a reported redox potential of 0.435 V vs SCE (Saturated calomel electrode) electrode to calibrate the pseudo reference electrode.<sup>6</sup> All the voltage profiles were then converted to be against an NHE (Normal hydrogen electrode) electrode. The tests in Ar were performed in the Ar-filled glovebox. The samples with saturated O<sub>2</sub> in the electrolyte were prepared by purging O<sub>2</sub> through the electrolyte for at least 5 minutes to reach a saturated condition for the electrolyte. These tests were conducted in the Ar-filled/O<sub>2</sub>-tolerant glovebox.

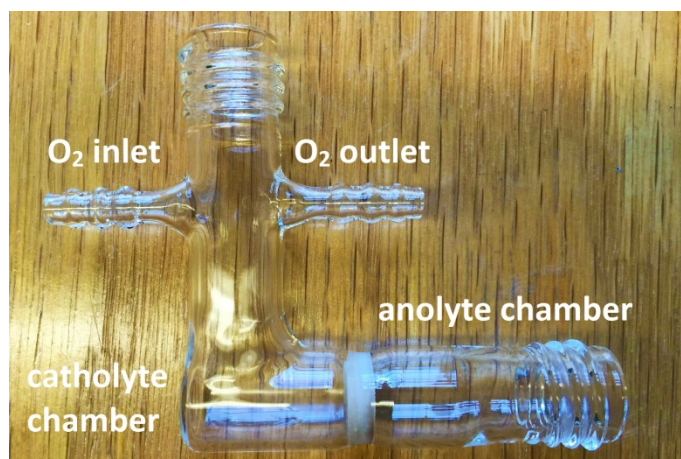


Fig. S2 Home-designed electrochemical cell for three-electrode measurements.

The cell was designed to carry out electrochemical measurements using catholyte and anolyte in separate chambers. A glass-frit as separator was applied in the middle connecting the separate chambers to minimize the crossover of the redox species and anions. The gas inlet and outlet could enable the flow of O<sub>2</sub> through the headspace of the catholyte chamber. Air tight sealing was ensured by rubber stopper cap and further by vacuum grease.

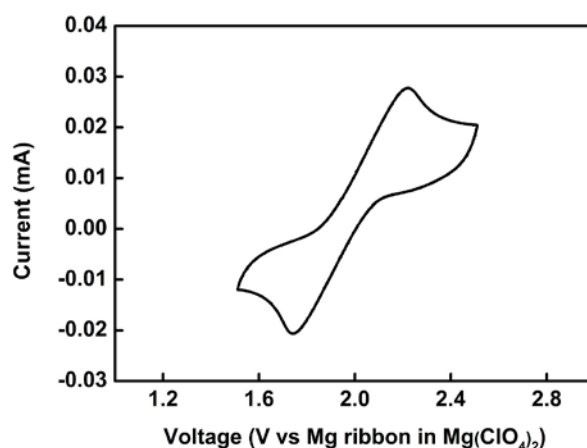


Fig. S3 Cyclic voltammetry (CV) to calibrate the Mg ribbon as the pseudo reference electrode.

Mg metal suffers severe passivation on the surface when immersed in various electrolytes. Therefore the calibration of the potential of Mg ribbon pseudo reference electrode in the anolyte by cyclic voltammetry (CV) was performed using the home-designed electrochemical cell.  $\text{Fc}^{+/0}$  redox couple was used as the internal reference redox pair in the catholyte with a reported redox potential of 0.435 V vs SCE electrode.<sup>6</sup>  $\text{Mg}(\text{ClO}_4)_2/\text{DMSO}$  electrolyte was applied as anolyte for this test as it was used for the galvanostatic cycling and CV measurements in the main text. Catholyte contained 2 mM Fc in  $\text{Mg}(\text{TFSI})_2/\text{DMSO}$  electrolyte. Pt wire and two pieces of polished Mg ribbons were used as working, counter and pseudo reference electrodes respectively in this experiment. By converting the voltage profile via the calibration and compare it with the  $\text{Mg}^{2+}/\text{Mg}$  redox couple (-2.37 V vs NHE), the passivation on the Mg surface accounted for a potential increment of 1.06 V. The potential of the Mg ribbon pseudo reference electrode (-1.31 V vs NHE) was also calibrated after the galvanostatic cycling and CV measurements. No distinct potential shift was observed.



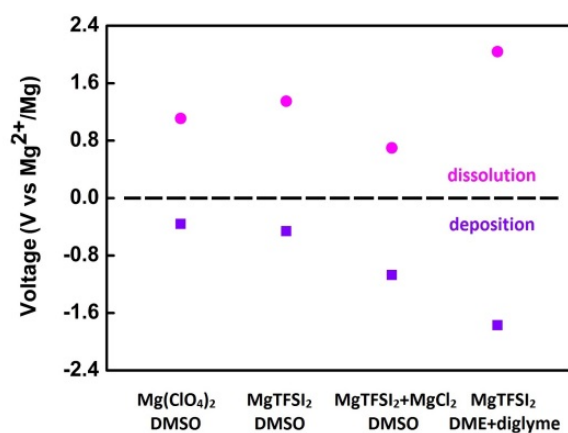


Fig. S4 Analyte screening with home-designed electrochemical cell.

The electrolyte composition was intensively studied in literatures to cope with the Mg dissolution and deposition chemistries. However, huge differences could be caused by the presence of O<sub>2</sub>. Therefore the analyte screening test was performed using the home-designed electrochemical cell. The concentration of each salt in the analyte was confined to 0.1 M. Catholyte contains 0.1 M Mg(TFSI)<sub>2</sub> in DMSO which is identical to the RM-free sample. Carbon paper and two pieces of polished Mg ribbons were applied as working, counter and pseudo reference electrodes respectively. The headspace of catholyte chamber was filled with O<sub>2</sub> prior to the measurements. Potentiostats (VMP3, Biologic) with a program (GPCL-2) that can monitor the working and counter electrode potentials simultaneously was applied for this set of experiments as well as for all other cycling profiles. During the cell operation, the cathode chemistry followed the oxygen reduction and evolution, while the anode chemistry was guided by Mg dissolution and deposition in various analyte compositions. The discharge and recharge states with equal capacities (0.1 mAh) for all the analytes were chosen to reflect their overpotentials. All the recorded voltage profiles were corrected to the Mg<sup>2+</sup>/Mg redox pair.

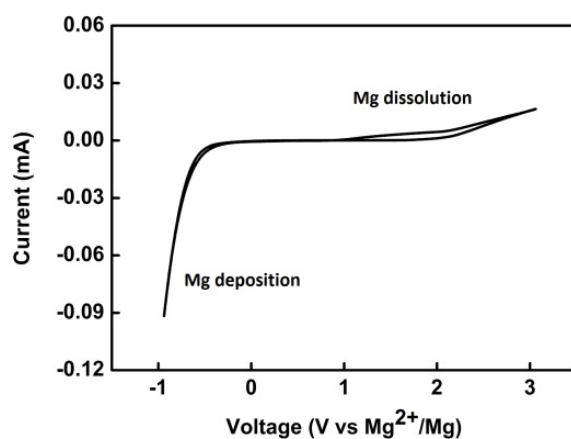


Fig. S5 Cyclic voltammetry (CV) of Mg electrode in  $\text{Mg}(\text{ClO}_4)_2/\text{DMSO}$ .

The cyclic voltammetry (CV) measurements were performed in the Ar-filled/ $\text{O}_2$ -tolerant glovebox with three-electrode configuration. Three pieces of polished Mg ribbons were applied as working, counter and pseudo reference electrodes respectively. The electrolyte contained 0.1 M  $\text{Mg}(\text{ClO}_4)_2$  dissolved in DMSO. The scan rate was confined to 25 mV/s. The recorded voltage profile was corrected to the  $\text{Mg}^{2+}/\text{Mg}$  redox pair. A large total overpotential can be observed even for the most optimal analyte choice. The overpotentials for Mg plating and stripping agree with the data shown in Fig. S4.

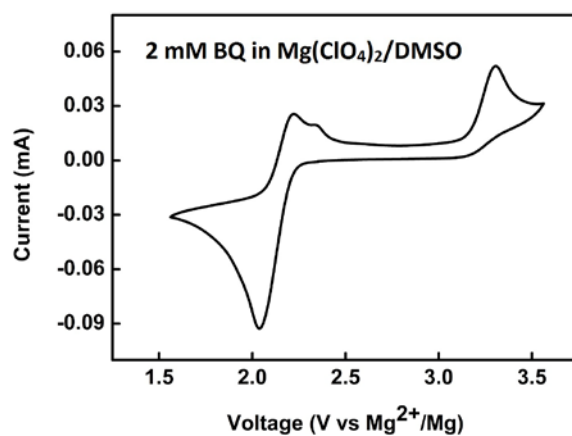


Fig. S6 Cyclic voltammetry (CV) of BQ in  $\text{Mg}(\text{ClO}_4)_2/\text{DMSO}$ .

The cyclic voltammetry (CV) measurement was performed in the Ar-filled glovebox with three-electrode configuration. Pt wire and two pieces of polished Mg ribbons were applied as working, counter and pseudo reference electrodes respectively. The electrolyte contained 0.1 M  $\text{Mg}(\text{ClO}_4)_2$  dissolved in DMSO. The scan rate was confined to 25 mV/s. The recorded voltage profile was corrected to the  $\text{Mg}^{2+}/\text{Mg}$  redox pair. Poor reversibility can be observed for  $\text{BQ}/\text{BQ}^{2-}$  redox pair with  $\text{Mg}(\text{ClO}_4)_2$ .

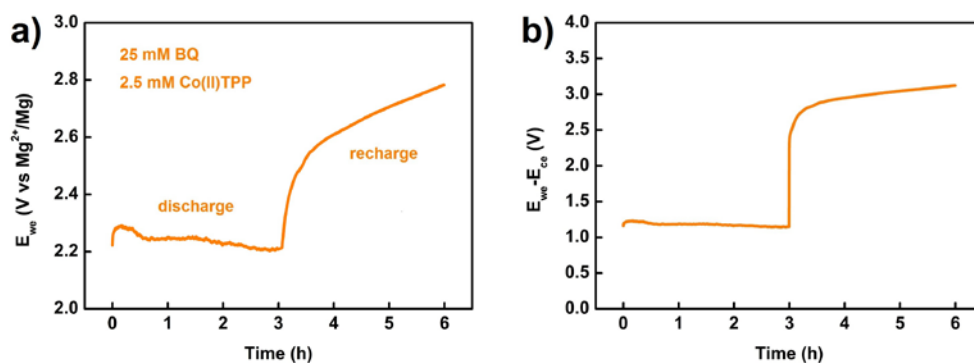


Fig. S7 Galvanostatic cycling using reduced concentrations of RMs. a) The voltage profile of the working electrode ( $E_{we}$ ) as measured against the Mg pseudo reference electrode. b) The voltage profile of the working electrode as measured against the counter electrode ( $E_{we}-E_{ce}$ ) in a two-electrode configuration.

The galvanostatic cycling was conducted to evaluate the influence of concentrations on the plateaus during discharge and recharge. No distinct shift of potentials can be observed when using 25 mM BQ and 2.5 mM Co(II)TPP (both reduced by half) while keeping the other parameters the same. However we expect a lower limit of the concentrations for both RMs to function when mass transport and kinetic factors become the limiting factor. The effect of concentrations of RMs will be further studied in the future. In order to avoid such confounding factors, we chose to use concentrations of 50 mM for BQ and 5 mM for Co(II)TPP based on their solubility in the electrolyte, for the measurement shown in Fig. 3.

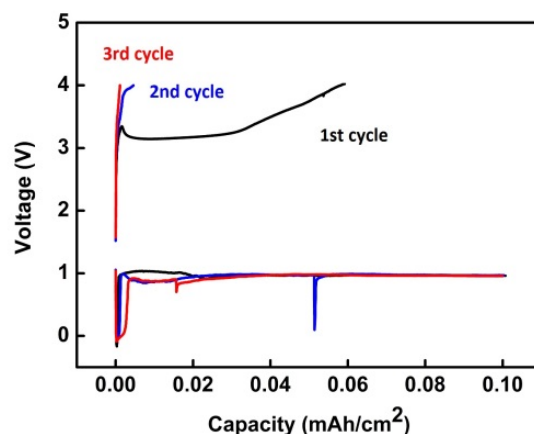


Fig. S8 Cycling performance in RMS-free  $\text{Mg}(\text{ClO}_4)_2/\text{DMSO}$  using a Swagelok cell in a two-electrode configuration (single chamber).

Customized Swagelok type cells were assembled in the Ar-filled glove box and further filled with  $\text{O}_2$  through the headspace in the Ar-filled/ $\text{O}_2$ -tolerant glovebox. An excess amount of polished Mg ribbon was applied as the anode. A piece of carbon paper with  $1.0 \text{ cm}^2$  area was used as cathode. A glass microfiber (GF/F Whatman) was chosen as the separator owing to its good compatibility and wettability with DMSO. The electrolyte was made of  $0.1 \text{ M Mg}(\text{ClO}_4)_2$  dissolved in DMSO due to the relatively low overpotentials. The current density for cycling was confined to  $0.02 \text{ mA/cm}^2$  for both discharge and recharge processes. The spikes during discharge could be ascribed to the sudden failure of the counter electrode such as complete surface passivation. Large initial polarizations might be required to clean the anode surface. Poor rechargeability and large voltage gaps between discharge and recharge could usually be observed when such a two-electrode configuration was used, which is in good agreement with other literature reports.<sup>7-9</sup>

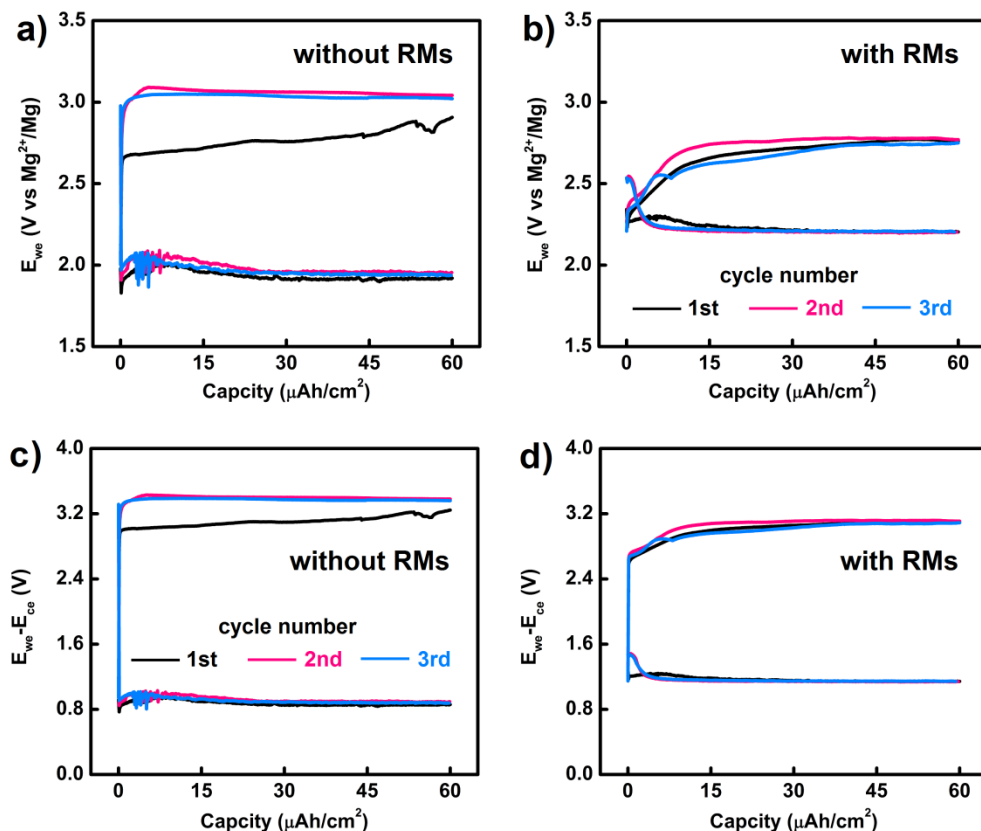


Fig. S9 Galvanostatic cycling plotted with capacity cutoff. a) The voltage profile of the working electrode ( $E_{we}$ ) as measured against the Mg pseudo reference electrode in RMs-free electrolyte. b) The voltage profile of the working electrode ( $E_{we}$ ) as measured against the Mg pseudo reference electrode in RMs-contained electrolyte. c) The voltage profile of the working electrode as measured against the counter electrode ( $E_{we}-E_{cc}$ ) in RMs-free electrolyte. d) The voltage profile of the working electrode as measured against the counter electrode ( $E_{we}-E_{cc}$ ) in RMs-contained electrolyte.

In addition to Fig. 3 in the manuscript, the performance of galvanostatic cycling can also be plotted by capacity cutoff for comparison. The cutoff value of  $60 \mu\text{Ah}/\text{cm}^2$  (corresponding to 3 h in each discharge and recharge step) equals approximately 10~20% of total capacity of the carbon paper cathode.

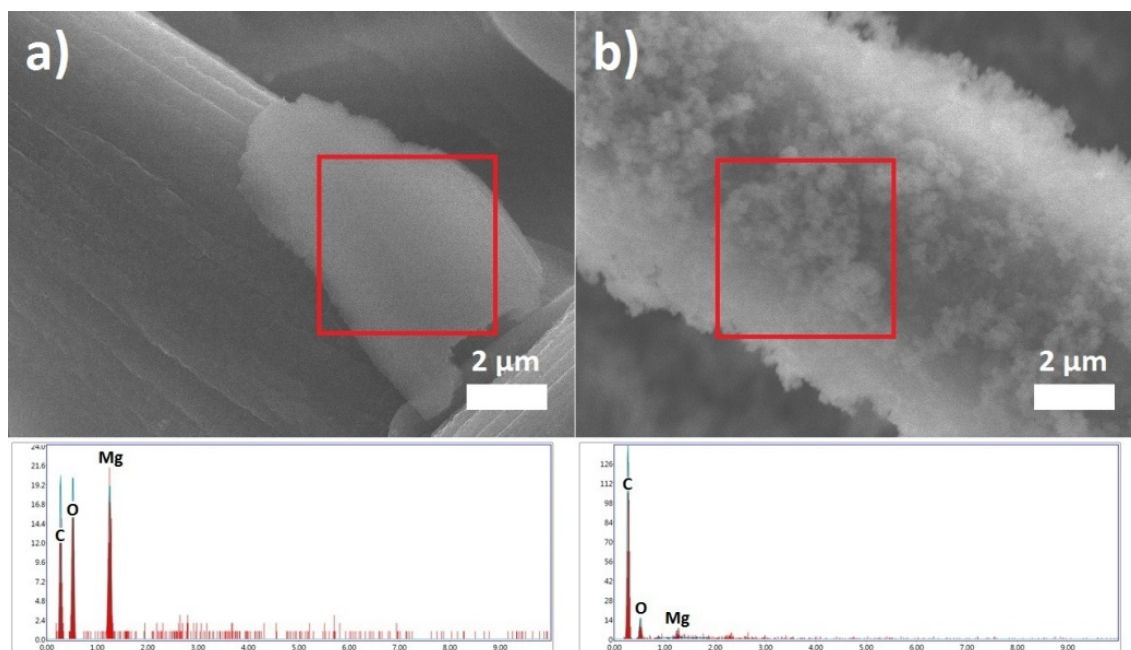


Fig. S10 SEM images and EDS spectra of the carbon paper cathodes after deep discharge. a) Carbon paper cathode after discharge to  $0.2 \text{ mAh/cm}^2$  in RMS-free electrolyte. b) Carbon paper cathode after discharge to  $0.2 \text{ mAh/cm}^2$  in RMS-contained electrolyte.

The carbon paper electrodes after discharged to  $0.2 \text{ mAh/cm}^2$  ( $0.2 \text{ mAh}$ , absolute capacity) were first soaked in DMSO to remove the salt and RMS, and then washed with acetone and isopropanol multiple times to further remove the solvent and RMS residues. The electrodes were then dried under vacuum at room temperature for 24 hours. The carbon signal came from the carbon paper electrode. The Mg and O signal confirmed the composition of the discharged product were Mg oxide mixtures in both cases. The strong carbon signal and relatively weak O and Mg signals were due to the well dispersed morphology of the small particles in the RMS-contained cell, which reduced the signal from the solid product. The absence of other signals (such as F, Cl and S) showed the cathode chemistry proceeded with the proposed route in discharge to form Mg oxide mixtures. Large particles (ca.  $10 \mu\text{m}$ ) were observed in RMS-free electrolyte while small particles (ca.  $200 \text{ nm}$ ) were observed in RMS-contained electrolyte.

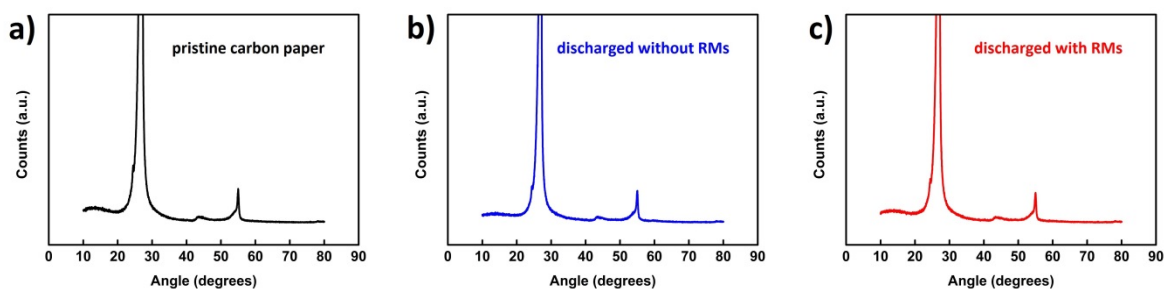


Fig. S11 XRD patterns of carbon paper cathodes after different operations. a) Pristine carbon paper cathode. b) Carbon paper cathode after discharge to  $0.2 \text{ mAh/cm}^2$  in RMs-free electrolyte. c) Carbon paper cathode after discharge to  $0.2 \text{ mAh/cm}^2$  in RMs-contained electrolyte.

This set of experiments was performed using the home-designed electrochemical cell. Anolyte contained  $0.1 \text{ M Mg(ClO}_4)_2/\text{DMSO}$ . Catholyte contained  $0.1 \text{ M Mg(TFSI)}_2/\text{DMSO}$  with or without RMs. Carbon paper and two pieces of polished Mg ribbons were applied as working, counter and pseudo reference electrodes respectively. The headspace of catholyte chamber was filled with  $\text{O}_2$  prior to the measurements. The pristine carbon paper electrode, carbon paper electrodes after discharged to  $0.2 \text{ mAh/cm}^2$  in RMs-free electrolyte and RMs-contained electrolyte were first soaked in DMSO to remove the salt and redox mediators, and then washed with acetone and isopropanol multiple times to further remove the solvent and redox mediator residues. The samples were finally dried under vacuum at room temperature for 24 hours and stored under Ar environment. XRD patterns showed no distinct difference between three cathode samples, indicating the discharge products in both discharged samples were of low crystallinity. The Y-axis was magnified for clarity. All the peaks can be ascribed to the pristine carbon paper electrode.



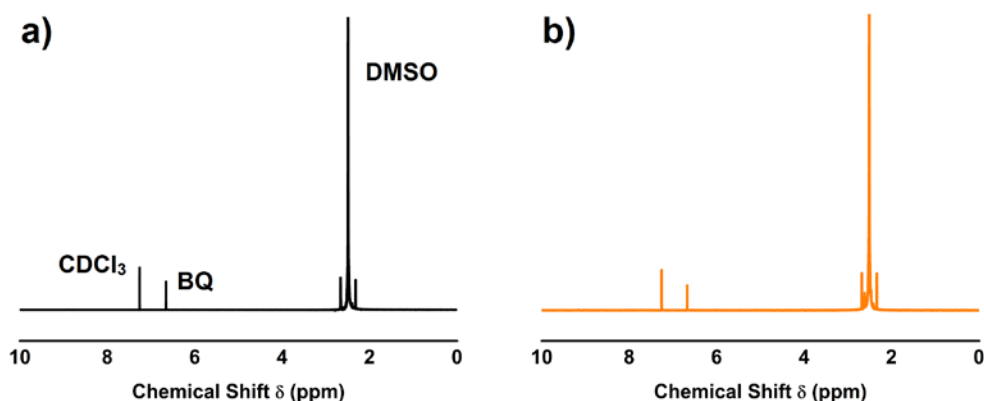


Fig. S12 NMR spectra of electrolytes before and after cycling. a) Electrolyte before cycling. b) Electrolyte after cycling.

This set of experiments was conducted using the home-designed electrochemical cell. Anolyte contained 0.1 M  $\text{Mg}(\text{ClO}_4)_2/\text{DMSO}$ . Catholyte contained 0.1 M  $\text{Mg}(\text{TFSI})_2/\text{DMSO}$  with RMs. Carbon paper and two pieces of polished Mg ribbons were applied as working, counter and pseudo reference electrodes respectively. The headspace of catholyte chamber was filled with  $\text{O}_2$  prior to the measurements. The samples were extracted by same amount from the catholyte before and after cycling, and were further dissolved in  $\text{CDCl}_3$ . The Y-axis was magnified for clarity. BQ exhibited good stability with almost no peak change before and after cycling. DMSO may have slightly decomposed upon cycling which may be one of the sources to account for the broadened C 1s XPS spectra after recharge in fig. S13. The instability of solvents is a common issue for metal-oxygen batteries. The Co(II)TPP species were undetectable by NMR due to its paramagnetic nature and low concentration in the electrolyte.

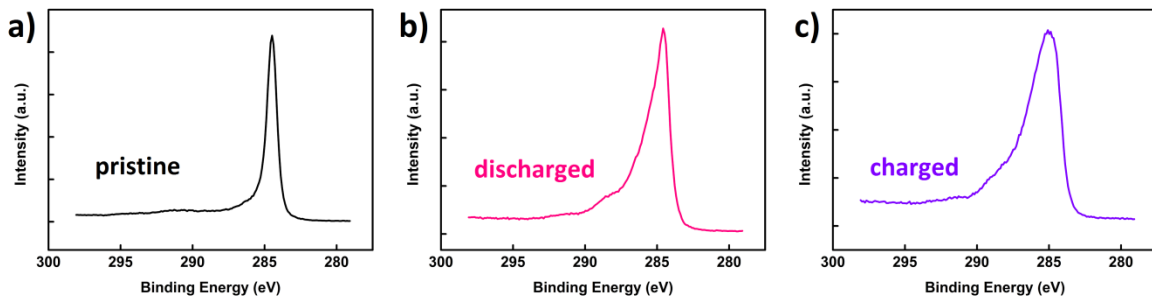


Fig. S13 XPS C 1s spectra of carbon paper cathodes after different operations. a) Pristine carbon paper cathode. b) Carbon paper cathode after discharge in the electrolyte with BQ and Co(II)TPP. c) Carbon paper cathode after full charge in the electrolyte with BQ and Co(II)TPP.

This set of experiments was performed using the home-designed electrochemical cell. Anolyte contained 0.1 M  $\text{Mg}(\text{ClO}_4)_2$  dissolved in DMSO. Catholyte contained 0.1 M  $\text{Mg}(\text{TFSI})_2$  dissolved in DMSO with RMs of BQ and Co(II)TPP. Carbon paper and two pieces of polished Mg ribbons were applied as working, counter and pseudo reference electrodes respectively. The headspace of catholyte chamber was filled with  $\text{O}_2$  before the measurements. The pristine carbon paper electrode, carbon paper electrodes discharged to  $0.2 \text{ mAh/cm}^2$  and fully charged in RMs-contained electrolytes were washed and dried following the previous procedure. A slight increase of oxidation state of the carbon paper electrode after discharge could be observed from the C 1s peak. After fully charged, an obvious broadened peak indicating more severe oxidation could be observed which was most likely due to the parasitic chemistries toward carbon paper electrode during the charging process. The instability of carbon based electrode was well known for metal-air batteries. The increase of oxygen content of carbon paper electrode could help explain the O residue after being fully charged as shown in Fig. 5b in the main text.

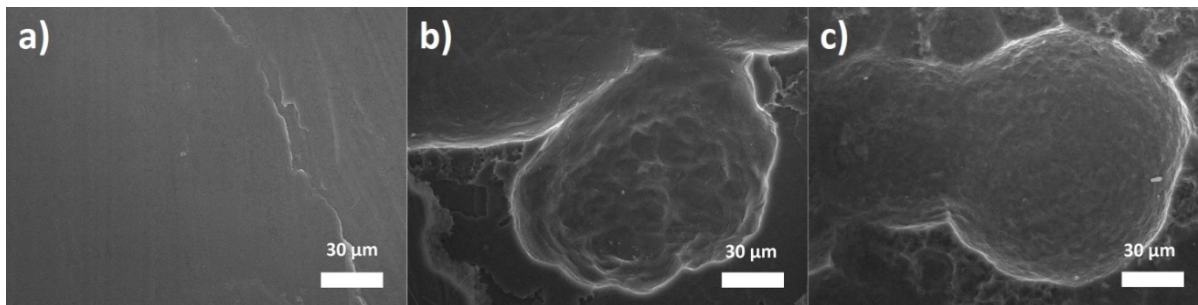


Fig. S14 SEM images of the Mg anodes after different operations in  $\text{Mg}(\text{ClO}_4)_2/\text{DMSO}$  electrolyte. a) Pristine Mg anode before use. b) Mg anode after discharge to 0.2 mAh. c) Mg anode after full charge.

This set of experiments was performed using the home-designed electrochemical cell. Anolyte contained 0.1 M  $\text{Mg}(\text{ClO}_4)_2/\text{DMSO}$ . Catholyte contained 0.1 M  $\text{Mg}(\text{TFSI})_2/\text{DMSO}$ . Carbon paper and two pieces of polished Mg ribbons were applied as working, counter and pseudo reference electrodes respectively. The headspace of catholyte chamber was filled with  $\text{O}_2$  prior to the measurements. The pristine Mg ribbon electrode, Mg ribbon electrodes after discharged to 0.2 mAh and fully charged in  $\text{Mg}(\text{ClO}_4)_2/\text{DMSO}$  electrolyte were first soaked in DMSO to remove the salt, and then washed with DME in the glovebox multiple times to further remove the solvent and salt residues. The samples were finally dried under vacuum at room temperature for 24 hours and stored under Ar environment. No dendritic growth could be found for the Mg ribbon electrode after the plating process.<sup>10,11</sup>

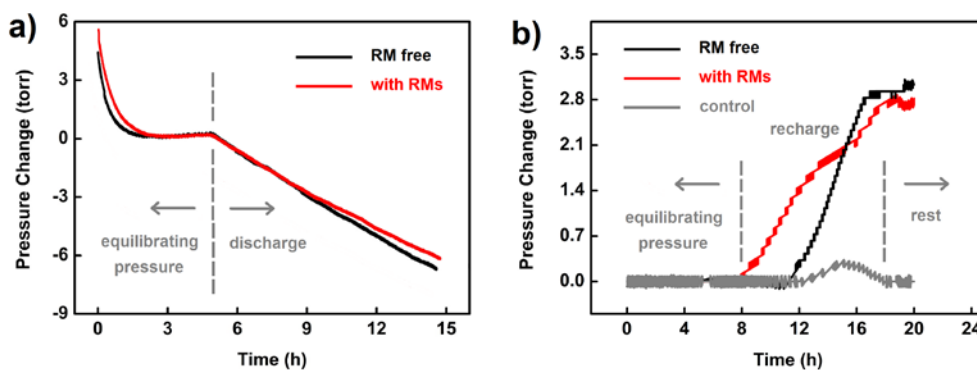


Fig. S15 Pressure change during discharge and recharge. a) Pressure change during discharge in the electrolytes with and without RMs. b) Pressure change during recharge in the electrolytes with and without RMs.

For the pressure monitoring tests, customized Swagelok type cells were first assembled in the Ar-filled glovebox using a pretreated Li (for recharge) or Mg ribbon (for discharge) as anode and a  $1.0 \text{ cm}^2$  preloaded (for recharge) or pristine carbon paper (for discharge and control sample for recharge) as cathode. The Swagelok type cells after assembly were then connected to the airtight pressure gauge, as detailed in our previous study.<sup>12</sup> With extended resting time to equilibrate the pressure, a stable baseline could be obtained which was further subtracted to show the absolute pressure change. The current density was confined to  $0.02 \text{ mA/cm}^2$  in both cases.

**Anode choices:** When single-chamber configuration was applied, the shuttling effect of RMs during recharge can be minimized by Li which possesses a solid electrolyte interface (SEI) layer as surface protection. Therefore the Li was applied as the anode for recharge. However the Li anode could not be applied for the discharge since the generated  $\text{Li}^+$  in the electrolyte will interfere with the cathode chemical reactions, thus the discharge and recharge were monitored separately. Although Mg is in direct contact with the RMs, the relatively large concentration of BQ and surface passivation of Mg will permit short-term pressure monitoring during discharge. Therefore our choice of anode materials for this set of experiment is justified. The surface pretreatment of Li by 0.1 M  $\text{LiNO}_3/\text{DMA}$  solution would help generate a stable artificial SEI layer to minimize the reaction between Li metal and the RMs. Nonetheless, the artificial SEI could not completely block such reactions, and the shuttling of RMs is to some extent inevitable.

**Electrolyte choices:** For recharge, the electrolytes were made of 0.1 M  $\text{LiClO}_4/\text{DME}$  with or without 2 mM  $\text{Co(II)TPP}$ . For discharge, the electrolytes were made of 0.1 M  $\text{Mg(ClO}_4)_2/\text{DMSO}$  with or without 50 mM BQ.

**Cathode choices:** For recharge process, the cells were operated with preloaded Mg oxide mixtures on carbon paper to mimic the cathode reactions as in the RMs-mediated  $\text{Mg-O}_2$  cells. A bare carbon paper cathode was used as control. For discharge process, pristine carbon papers were applied.

The pressure monitoring experiments were less than ideal due to the parasitic chemistries involved. However the *in situ* gas consumption and evolution shown by pressure profile served as a semi-quantitative evidence to support the high efficiency of BQ and  $\text{Co(II)TPP}$  as RM for the cell operations in both discharge and recharge processes.

## References

- (1) M. J. Lacey, J. T. Frith and J. R. Owen, *Electrochem. Commun.* 2013, **26**, 74–76.
- (2) N. Feng, P. He and H. Zhou, *ChemSusChem* 2015, **8**, 600–602.
- (3) S. Matsuda, S. Mori, K. Hashimoto and S. Nakanishi, *J Phys. Chem. C* 2014, **118**, 28435–28439.
- (4) E. R. Milaeva, G. Speier and A. B. Lever. No. TR-45. YORK UNIV NORTH YORK (ONTARIO) DEPT OF CHEMISTRY, 1992.
- (5) D. Sun, Y. Shen, W. Zhang, L. Yu, Z. Yi, W. Yin, D. Wang, Y. Huang, J. Wang, D. Wang and J. B. Goodenough, *J Am. Chem. Soc.* 2014, **136**, 8941–8946.
- (6) J. Aranzaes Ruiz, M.-C. Daniel and D. Astruc, *Can. J. Chem.* 2006, **84**, 288–299.
- (7) G. Vardar, E. G. Nelson, J. G. Smith, J. Naruse, H. Hiramatsu, B. M. Bartlett, A. E. S. Sleightholme, D. J. Siegel and C. W. Monroe, *Chem. Mater.* 2015, **27**, 7564–7568.
- (8) T. Shiga, Y. Hase, Y. Kato, M. Inoue and K. Takechi, *Chem. Commun.* 2013, **49**, 9152–9154.
- (9) T. Shiga, Y. Hase, Y. Yagi, N. Takahashi, K. Takechi, *J Phys. Chem. Lett.* 2014, **5**, 1648–1652.
- (10) C. Ling, D. Banerjee and M. Matsui, *Electrochim. Acta* 2012, **76**, 270–274.
- (11) M. Matsui, *J Power Sources* 2011, **196**, 7048–7055.
- (12) X. Yao, Q. Cheng, J. Xie, Q. Dong and D. Wang, *ACS Appl. Mater. Inter.* 2015, **7**, 21948–21955.